

Effect of frictional boundary conditions and percentage area reduction on the extrusion pressure of Aluminum AA6063 alloy using FE analysis modelling

Sunday Temitope Oyinbo^a, Tien-Chien Jen^{a*} and Sikiru O. Ismail^b

^aDepartment of Mechanical Engineering Science, University of Johannesburg, Gauteng, 2006, South Africa

^bSchool of Engineering and Computer Science, University of Hertfordshire, United Kingdom

ARTICLE INFO

Article history:

Received 23 September 2019

Accepted 21 January 2020

Available online

21 January 2020

Keywords:

Deformation Analysis

Extrusion Pressure

Friction factor

Deform™-3D

Percentage Reduction

ABSTRACT

Finite Element Analysis was carried out to describe the effect of frictional boundary conditions and percentage reduction on deformation modelling (forward extrusion) of Aluminum AA6063 alloy. Curved die profiles of regular polygons (square, hexagonal, heptagonal, and octagonal) were designed using MATLAB R2009b and Autodesk Inventor 2013 to generate the coordinate and the solid CAD model of the die profile respectively form a circular billet. The numerical analysis was performed using Deform™-3D commercial package with frictional boundary conditions of 0.38 and 0.75 representing the wet and dry condition and varying the percentage reduction of 50%, 70%, and 90%. The results of the temperature distribution, effective stress, effective strain, and strain rate were reported. As the percentage area reduction increases, the extrusion pressure also increases with an increasing frictional condition, and die length. Also, extrusion pressure decreases when the side of the polygon increases from square-shaped section follow by hexagonal shaped-section and least in octagonal shaped-section for both friction factors and percentage area reductions. For a given percentage reduction and cross-sectional area, there is no distinct difference between the predictive loads for the shaped-polygons. When the result of this analysis is compared with the experimental results from the literature, it is evident that Deform™-3D is an effective tool for finite element analysis of non-isothermal deformation processes.

© 2020 Growing Science Ltd. All rights reserved.

1. Introduction

The demand for metal forming operations has increased rapidly due to the advancement in technological growth and industrialization. This process offers several advantages in contrast to the requirements of other manufacturing processes in terms of reduction in material wastage (scraps) as well as improved the products' mechanical properties. The extrusion process in massive metal deformation plays a vital role by reducing the billets' cross-sectional area when forced through a die by a ram (Flitta et al., 2007; Solomon & Solomon, 2010; Altinbalik & Ayer, 2013). Materials such as metals, polymers, foodstuffs, ceramics and concretes are commonly extruded. Aluminium alloy can be extruded as well as alloys of tin, copper, steel, lead etc. This research examines the effect of boundary conditions and percentage area reduction on the extrusion pressure using aluminium AA6063 alloy. Aluminum AA6063 alloy can be hot or cold extruded. The shape of the extruded products can be greatly affected by various parameters due to the way material flows through the die. Several internal variables such as deformation

* Corresponding author.
E-mail addresses: tjen@uj.ac.za (T.C. Jen)

temperature, billet metallurgical structure and chemical composition, prior strain history and segregation, deformation rate, shape factor, boundary frictional condition, and grain size influence extrusion process during deformation, therefore a complex process (Oyinbo et al., 2015; Alam et al., 2016).

Because of the manufacturing simplicity and convenience, shear faced die is preferred in most forming industries for the extrusion process, but a lot of redundant work is produced in the process thereby decreases the efficiency of the process and increases the power required for metal deformation. To overcome this challenge of energy loss, Maity et al.,(1996) investigated square to square extrusion process using the various design of curved die and friction factors. The die geometry was optimized using appropriate process parameters. They obtain a lower extrusion pressure when cosine die profile was used. In the case of sticking-friction conditions, the straight tapered die was used with upper bound analysis to achieve optimized results.

The effects of various lubricating conditions were investigated by Ikumapayi et al., (2019) on aluminium AA6063 alloy during the backward cup extrusion process to determine the temperature distribution during deformation. Different lubricants were used at different strain rates. The result of their finding was also compared with numerical analysis which shows that during deformation, the increasing strain rates increase the temperature both at the lower die and punch interface. Also, when tropical coconut oil was used as the lubricating oil at a higher strain rate, the highest temperature was recorded as compared with other lubricants. Ajiboye & Oyinbo,(2014) numerically simulated extrusion of various shapes ranging from simple to advance polygons using Deform 3D, a solid CAD model from a round billet. Dry and lubricated conditions were observed to determine the extrusion load. It was discovered that predictive loads for simple shapes are lower than that of advance polygons and there was a significant reduction in the extrusion load during lubricating conditions.

Shear extrusion process was used to study aluminium alloy AA6063 in other to determine the forming load using variables such as die diameter, punch land and lubricants by Ojo et al., (2015). They found out that a punch with small punch land and with the large diameter is best for material forming during shear backward cup extrusion. Also, the effects of various lubricants were also examined to determine the stress distribution and extrusion load during deformation. Palm oil shows minimum load during the process. Ajiboye et al., (2014) investigated the effects of environmentally friendly lubricants on aluminium alloy AA6063 to improve its mechanical properties during equal channel angular extrusion (ECAE). It was observed that the maximum ductility and ultimate tensile strengths with the least extrusion pressure were obtained when palm oil lubricant was used. Palm and olive oil yields the least deformation load than others, Furthermore, greater hardness and higher homogeneity were observed within the rod at the tensile stain side than the compressive side. The present study reports on the relationship between the frictional boundary conditions, percentage area reduction and deformation characteristics of forward extrusion of Aluminum AA6063 alloy using the DeformTM-3D simulation software.

2. Solid Model design

In this present research, parametric mathematical equations were derived for curved die profiles of various shaped-sections from a circular billet. The shaped-sections are square, hexagonal, heptagonal and octagonal section. Afterwards, the co-ordinate of the die profile was generated using MATLAB R2009b. Autodesk Inventor 2013 commercial package was used to produce the solid CAD of the curved die profile. Fig. 1 shows the CAD model for extrusion of the regular polygons (square, hexagonal, heptagonal and octagonal) profile from a circular billet. The solid CAD models are developed for 50%, 70% and 90% area reduction and the length are given to be 50mm

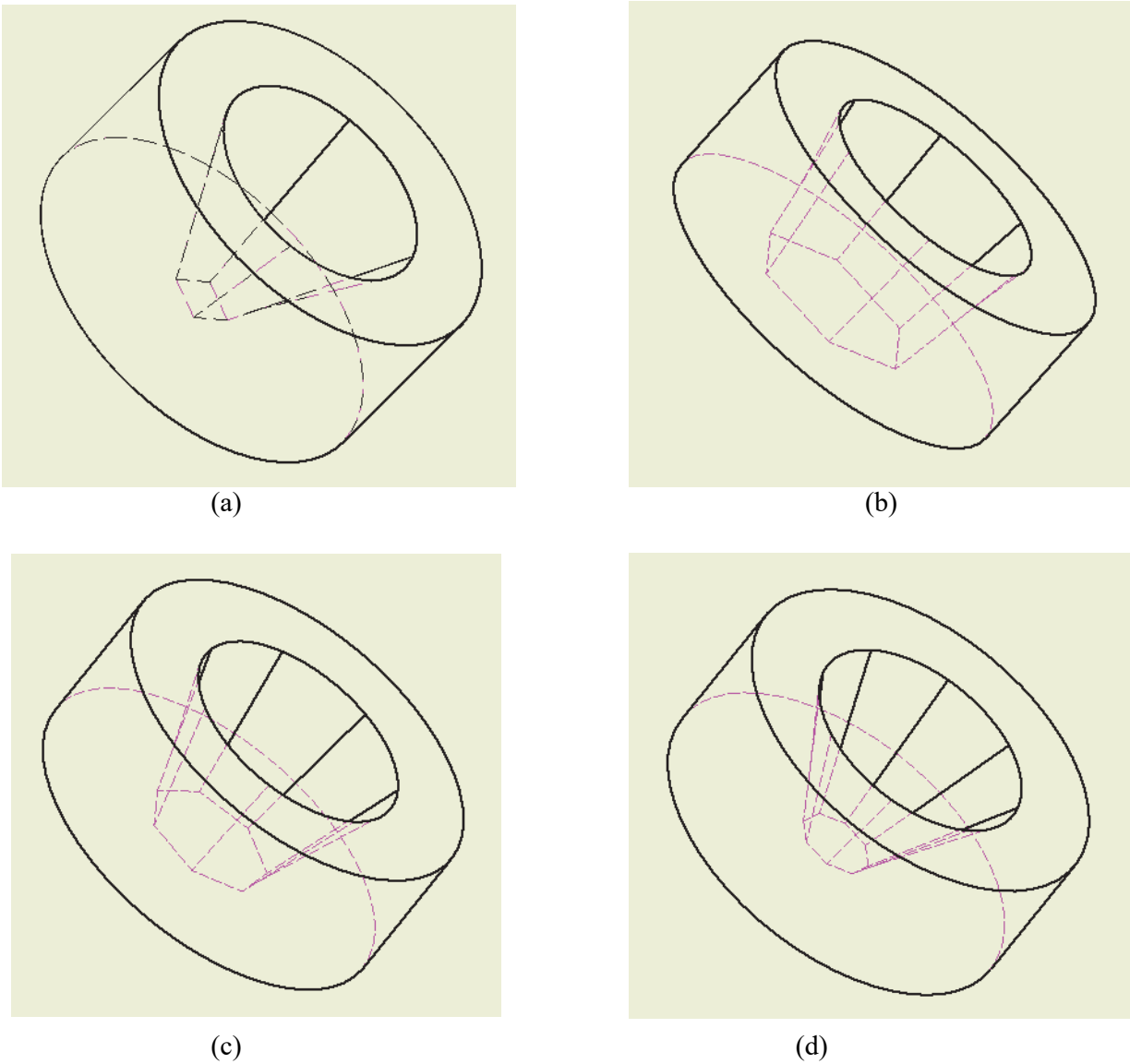


Fig. 1. Extrusion die profile for (a) square- section at 90% reduction (b) hexagonal-section at 50% reduction (b) heptagonal-section at 70% reduction (c) octagonal-section at 90% reduction

3. Numerical modelling

The Finite Element Analysis (FEA) is a computational tool used for modelling and simulation of a variety of complex engineering problems. In the metalworking industry, DeformTM-3D software is applied to simulate and analyze the metal flow characteristics. The DeformTM-3D commercial package is used for the actual finite element analysis of the extrusion process to study the deformation process and the behaviour of the deformed. DeformTM-3D is an effective tool for finite element analysis of non-isothermal deformation processes because the software is based on FE formulation of rigid-plastic and it is capable of handling multiple billets and die. The numerical calculations needed for solving the problem during the analysis are performed by this simulation engine (DEFORM TM 3D Version 6.1, 2008). The rigid curved die was modelled in this study for the extrusion of square, hexagonal, heptagonal, and octagonal shaped-section with rigid plastic circular billet. Tetrahedral solid elements were used for the meshing as shown in Fig. 2 with the mesh automatically generated in the model. The frictional factor formulation was used with $\mu_{wet} = 0.38$ and $\mu_{dry} = 0.75$ as determined from the ring compression test. The material of the circular workpiece (billet) is taken as aluminium AA6063 alloy. The simulation was

carried out at room temperature. The calculation plan used to study the effects of parameters for extrusion simulation process is shown in Table 1. Similar conditions were used in our previous study (Ikumapayi et al., 2019; Oyinbo et al., 2015) are summarized in Table 1.

Table 1. Schematic Calculation plan used in the simulation to study the effects of parameters

A. Parametric Outline						
Parameters Inputs	Temperature 30°	Strain Rate 0.025s^{-1}	Ram Speed 0.075 mm/s	Friction factor 'm' 0.38 and 0.75		
B. Details of individual component						
Name of parts	Dimension of the part (mm)		Materials			
	Cross-section	Length				
Billet	$\phi 60$	80	Aluminum alloy 6063			
Punch	$\phi 60$	120	Rigid			
Bottom die with opening	$\Phi 100$ external $\Phi 60$ internal	40~50	Rigid			
Ram	$\Phi 100$ external $\Phi 60$ internal	100	Rigid			
C. Aluminum material properties						
Thermal Conductivity (w/m-k)	218					
Thermal Expansion ($10^{-6}/^{\circ}\text{C}$)	23.4					
Tensile Strength (MPa)	90.0					
Elastic Modulus (GPa)	70.0–80.0					
Poisson's Ratio	0.330					
Density ($\times 1000\text{kg/m}^3$)	2.70					
Fatigue Strength (MPa)	55.0					
Shear Strength (MPa)	69.0					
Hardness (HB500)	25.0					
Yield Strength (MPa)	48.0					

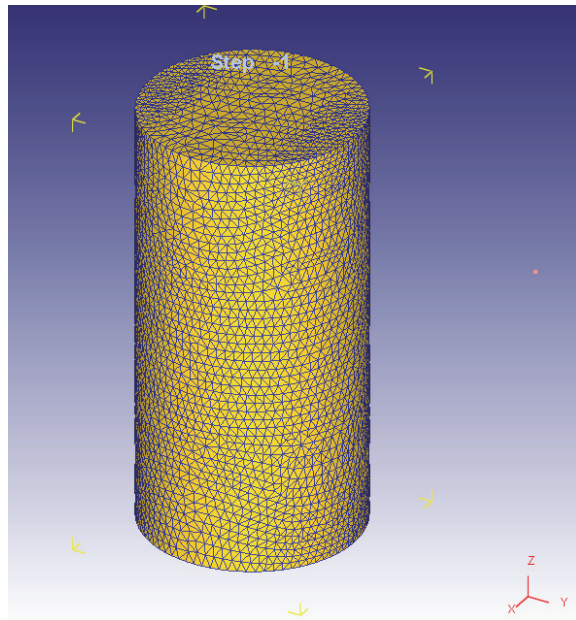


Fig. 2. The finite element model showing the meshed cylinder for the simulation process (Number of elements =50000)

4. Results and discussion

4.1. The deformation profile of the extruded shaped-section from circular billet

The deformation of the materials in the whole process changes from one phase to another when the billet is squeezed through a die as a common phenomenon to engineering materials. The deformation is fully plastic from a region of elastic-plastic but at the beginning, it was purely elastic. The deformation of extruded aluminium from the typical 3D-numerical simulation results is compared with the typical experimental observation (Rout et al., 2017). From the present investigation, temperature distribution, the evolution of effective stress, strain rate and effective strain are reported for curved die profile at a percentage area reduction of 90% and frictional boundary conditions ($\mu_{wet} = 0.38$). Figs. 3 to 6 show the above parameters for extrusion of hexagonal shaped-section from round billet as computed from FEM modelling. During extrusion, certain factors are responsible for generating heat at the deformation zone. These factors are the deformation of the billet (workpiece), friction at the billet-die interfaces, and shearing at the boundary of deformation region. Some of the generated heat is conveyed into the deformed material, some are transported into the die and container, and some leads to billet temperature rise. Die land experiences higher temperature than at the dead metal zone. This is because more heat is generated at the die land region due to the frictional pressing work being translated into heat at this region which gives rise to a rapid increase in temperature above the temperature rise at dead metal zone (Fig. 3) (Ajiboye & Adeyemi, 2007; Ajiboye & Adeyemi, 2008). Hence, it can be observed that as the polygon side increases, the maximum temperature generated decreases at an indicated frictional factor and percentage area reduction (Fig. 3 (a)-(d)). Fig. 4 shows the variation of the stress distribution in the deformed billet at different shaped-sections. The effective stress decreased with the increase in the size of the polygon as shown in Figs. 4(a)-(d). Fig. 5 and Fig. 6 show the shape of the billet after deformation and variation of the strain distribution behaviour and strain rate at an indicated frictional factor and percentage area reductions respectively. At lower strain rate there are higher frictional forces due to a longer contact between the die and the workpiece. The frictional forces lead to change in the deformation temperature and impede plastic deformation, thereby causing heterogeneous deformation (Rasti et al., 2011). The results further indicated that the strain distribution varies across the deformed sample (Fig. 6 (a)-(d)). As shown, higher deformation was experienced at the centre of the deformed at all shaped section. This region experienced an intense shearing of the microstructure leading to severe plastic deformation. Under this condition, refinement of the grain structure may occur due to dynamic recrystallization softening mechanism (Zhang et al., 2009).

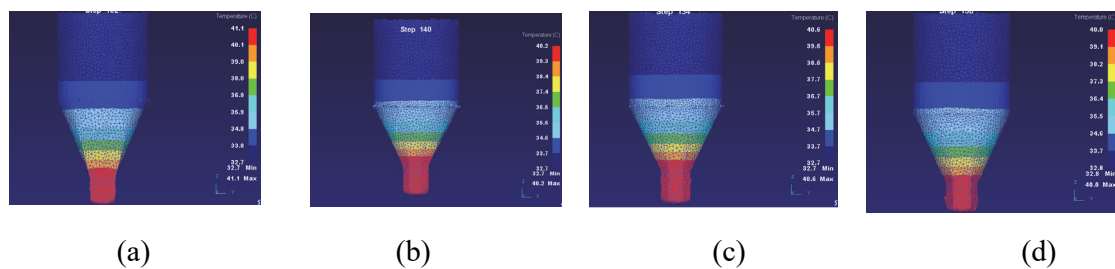


Fig. 3. Temperature distribution for 90% reduction and $\mu = 0.38$ (a) square-section (b) hexagonal-section (c) heptagonal-section (d) octagonal-section

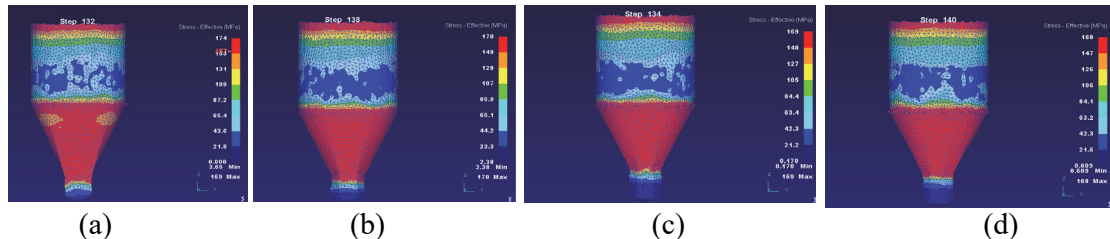


Fig. 4. Effective-stress analysis for 90% reduction and $\mu = 0.38$ (a) square-section (b) hexagonal-section (c) heptagonal-section (d) octagonal-section

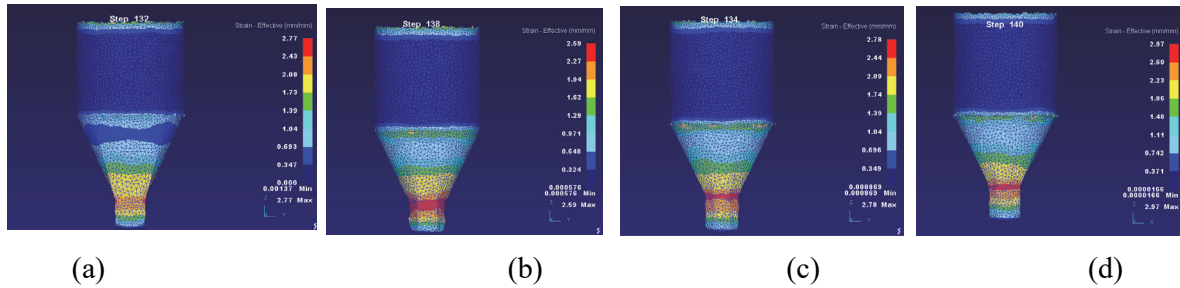


Fig. 5. Effective-Strain analysis for 90% reduction and $\mu = 0.38$ (a) square-section (b) hexagonal-section (c) heptagonal-section (d) octagonal-section

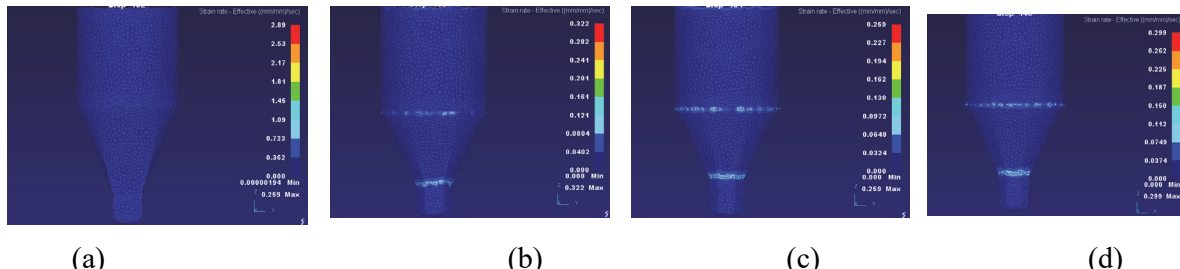


Fig. 6. Effective-Strain rate analysis for 90% reduction and $\mu = 0.38$ (a) square-section (b) hexagonal-section (c) heptagonal-section (d) octagonal-section

4.2. The effect of boundary frictional conditions and percentage area reduction on the extrusion pressure

The effective load prediction versus punch displacement of the curved die profile of square, hexagonal, heptagonal and octagonal cross-section from circular billet for 90% reduction and lubricated condition ($\mu_{wet} = 0.38$), are shown in Fig. 7 (a)-(d), respectively.

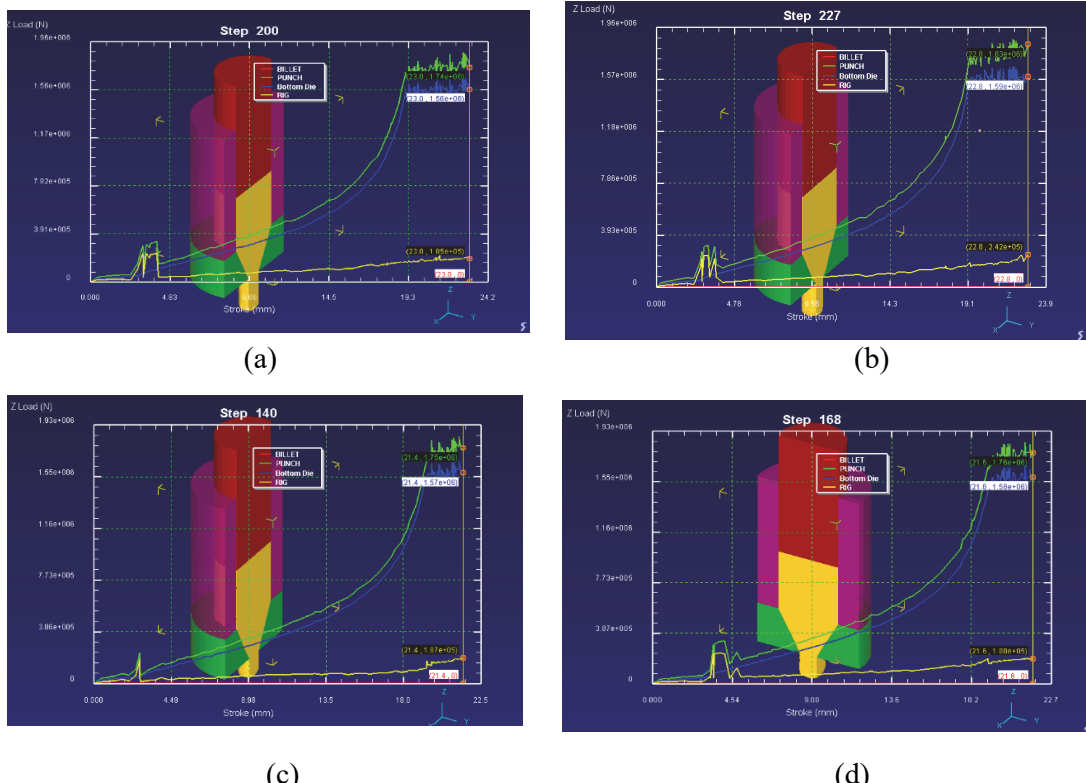
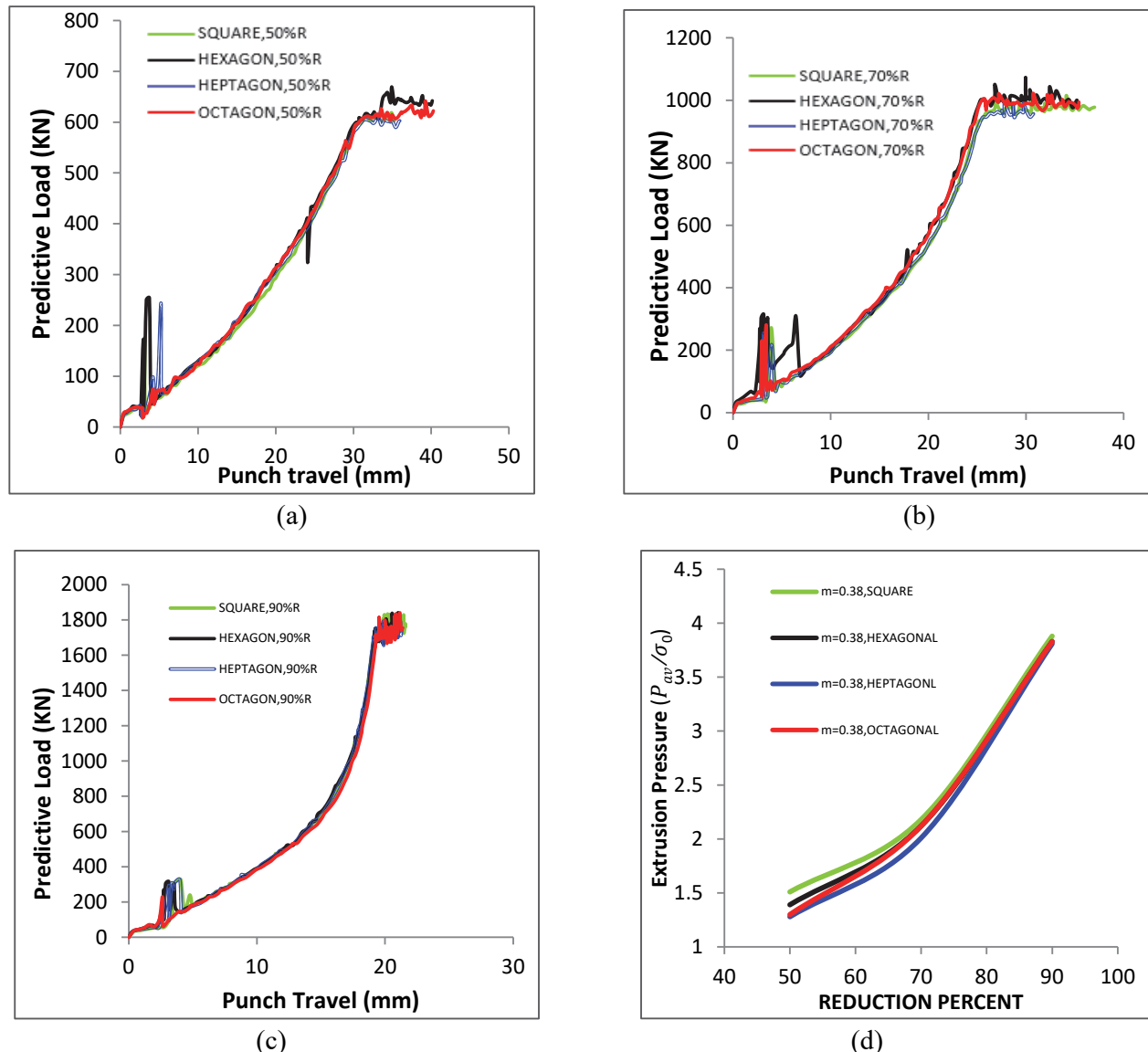
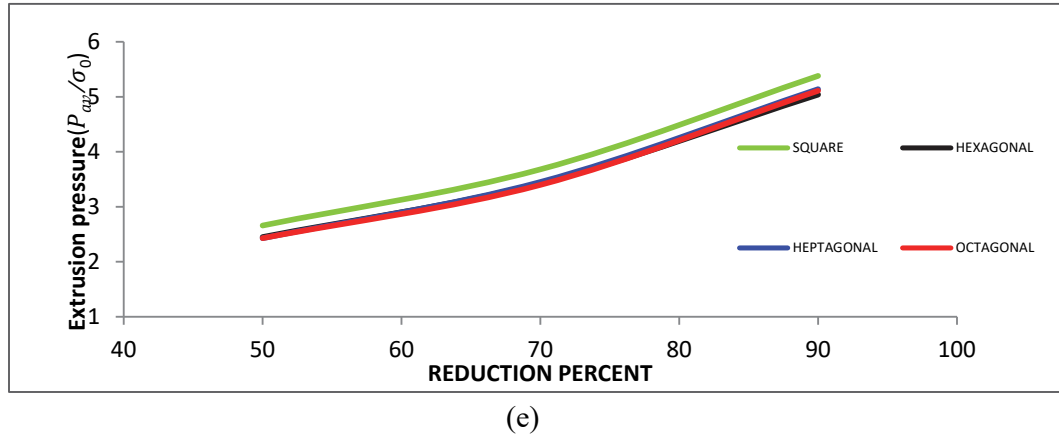


Fig. 7. Variation of predictive load with respect to punch displacement of (a) square-section (b) hexagonal-section (c) heptagonal-section and (d) octagon-section for 90% reduction and $\mu = 0.38$

The effective load on all the components, such as the bottom die, the container, the punch and the workpiece (billet), involved are shown in Fig. 7. It is observed that the punch experiences the highest load in all the graphs follow by the bottom die and then the container (rig) while billet absorbed the least load during the operation. Also, the wavy nature as observed in the graph is due to the initial filling of the billet into the die. This wavy nature becomes more and more visible as the complexity of the die profile increases. The container shows more of this behaviour while billet deformation and the bottom die show the least. The tool live span is likely to be affected by this wavy observation. Fig. 8 (a)-(d) shows the predictive loads versus stroke curves for aluminium AA6063 alloy of the curved die profile of square, hexagonal, heptagonal and octagonal cross-section from circular billet for 90% reduction and lubricated condition ($\mu_{wet} = 0.38$) at room temperature. Also, extrusion pressure is shown in Fig. 8 (d)-(e) with respect to the percentage area reduction and friction factor ($\mu_{wet} = 0.38$) of the curved die profile. It can be observed that as the polygon side increases, extrusion pressure decreases both in the case of friction factors and indicated percentage area reduction (Fig. 9). This is because the metal flows easily through the die profile as the shape of exit die geometry is approaching the shape of entry geometry and moreover the design of the die cross-section is to gradually reduce from circular to the exit polygon (Onawola & Adeyemi, 2003; Rout et al., 2017). The Square curved die has highest extrusion pressure, followed by hexagonal and octagonal shaped-section has the least (Fig. 9). In the case of predictive load, there is no marked difference between the polygons.





(e)

Fig. 8. Comparison of (a) predictive load versus punch displacement of different geometry at 50% area reduction (b) predictive load versus punch displacement of different geometry at 70% area reduction (c) predictive load versus punch displacement of different geometry at 90% area reduction (d) Extrusion pressure versus percentage area reduction at ($\mu=0.38$) (e) Extrusion pressure versus percentage area reduction at ($\mu=0.75$)

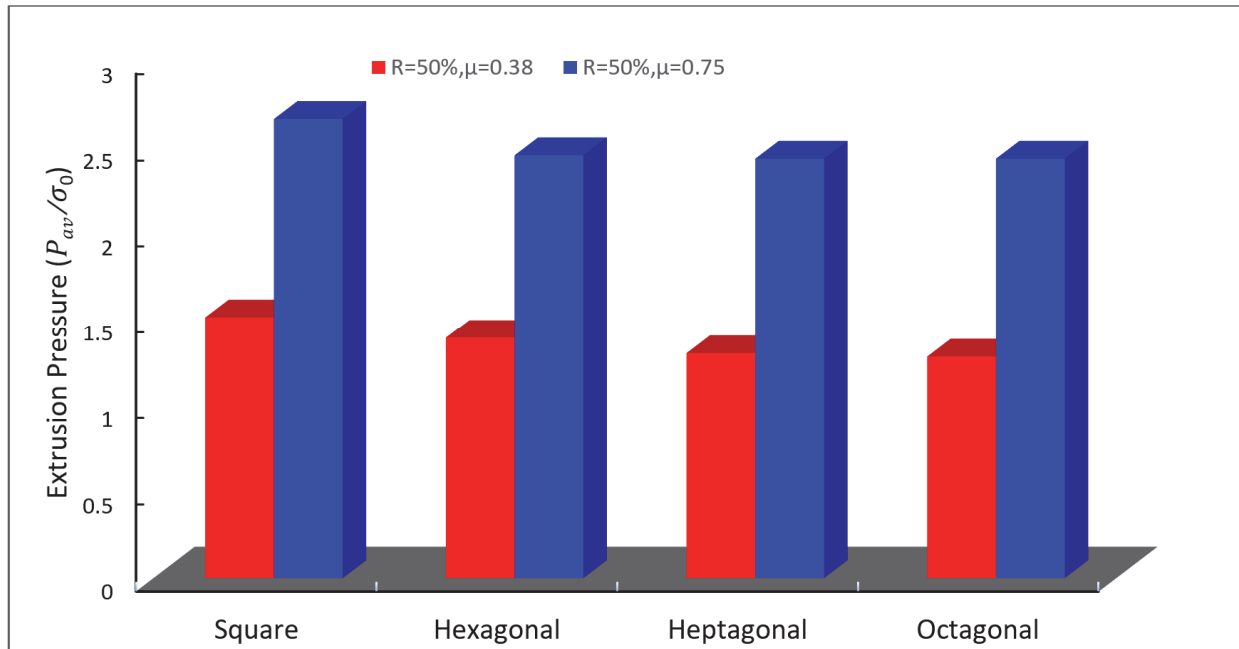


Fig. 9. Extrusion Pressure for various polygon at the reduction of 50% and varying friction factor

5. Conclusion

From the simulation of the extrusion process using Deform™-3D commercial package and Aluminium AA6063 alloy as workpiece with frictional boundary conditions of 0.38 and 0.75 and varying percentage reduction of 50%, 70%, and 90%, the following conclusions were drawn

- The temperature, effective stress, effective strain, effective-strain rate distribution during extrusion simulation of the billet exhibited an inhomogeneous behaviour across the deformed cross-section of the cylindrical billet. The inhomogeneity behaviour can be attributed to the change in the deformation temperature and the effect of the friction at the curved die-billet contact interface.

- It is found that as the side of the considered polygon increases, the extrusion pressure decreases for both friction factors at the indicated percentage area reductions. The extrusion pressure is higher in square shaped-section, while there is no marked difference between the predictive loads for the polygons at a given percentage reduction and cross-sectional area (Rout et al., 2017).

References

- Ajiboye, J. S., & Adeyemi, M. B. (2007). The effect of selected parameters on temperature distribution in axi-symmetric extrusion process. *Journal of Mechanical Science and Technology*, 21(10), 1553–1559. <https://doi.org/10.1007/BF03177374>
- Ajiboye, J.S., & Adeyemi, M. B. (2008). Effects of extrusion variables on temperature distribution in axisymmetric extrusion process. *International Journal of Mechanical Sciences*, 50(3), 522–537. <https://doi.org/10.1016/J.IJMECSCI.2007.08.006>
- Ajiboye, J.S., & Oyinbo, S. T. (2014). Load Prediction for the Extrusion from Circular Billet to Symmetric and Asymmetric Polygons Using Linearly Converging Die Profiles. *Key Engineering Materials*, 622–623, 119–128. <https://doi.org/10.4028/www.scientific.net/KEM.622-623.119>
- Ajiboye, Joseph S., Adebayo, S. A., & Azeez, T. M. (2014). Effects of lubricant on the mechanical properties of aluminum 6063 alloy after ECAE. *Industrial Lubrication and Tribology*, 66(3), 360–364. <https://doi.org/10.1108/ilt-10-2011-0076>
- Alam, M. S., Kaur, J., Khaira, H., & Gupta, K. (2016). Extrusion and Extruded Products: Changes in Quality Attributes as Affected by Extrusion Process Parameters: A Review. *Critical Reviews in Food Science and Nutrition*, 56(3), 445–473. <https://doi.org/10.1080/10408398.2013.779568>
- Altinbalik, T., & Ayer, O. (2013). Effect of die inlet geometry on extrusion of clover sections through curved dies: Upper bound analysis and experimental verification. *Transactions of Nonferrous Metals Society of China (English Edition)*, 23(4), 1098–1107. [https://doi.org/10.1016/S1003-6326\(13\)62571-6](https://doi.org/10.1016/S1003-6326(13)62571-6)
- DEFORM TM 3D Version 6.1. (2008). In (sp2), *User's Manual Scientific Forming Technologies Corporation*, 2545 Farmers Drive, Suite200, Columbus, Ohio, 43235.
- Flitta, I., Sheppard, T., & Peng, Z. (2007). FEM analysis to predict development of structure during extrusion and subsequent solution soak cycle. *Materials Science and Technology*, 23(5), 582–592. <https://doi.org/10.1179/174328407X158668>
- Ikumapayi, O.M., Oyinbo, S. T., Bodunde, O. P., Afolalu, S. A., Okokpugie, I. P., & Akinlabi, E. T. (2019). The effects of lubricants on temperature distribution of 6063 aluminium alloy during backward cup extrusion process. *Journal of Materials Research and Technology*, 8(1). <https://doi.org/10.1016/j.jmrt.2018.08.006>
- Maity, K. P., Kar, P. K., & Das, N. S. (1996). A class of upper-bound solutions for the extrusion of square shapes from square billets through curved dies. *Journal of Materials Processing Technology*, 62(1–3), 185–190. [https://doi.org/10.1016/0924-0136\(95\)02228-7](https://doi.org/10.1016/0924-0136(95)02228-7)
- Ojo, S. O., Erinoshio M., & Ajiboye, J. S. (2015). Experimental Analysis for Lubricant and Punch Selection in Shear Extrusion of Aa-6063. *J Material Sci Eng*, 4(4), 174. <https://doi.org/10.4172/2169-0022.1000174>
- Onawola, O. O., & Adeyemi, M. B. (2003). Warm compression and extrusion tests of aluminium. *Journal of Materials Processing Technology*, 136(1–3), 7–11. [https://doi.org/10.1016/S0924-0136\(02\)00462-4](https://doi.org/10.1016/S0924-0136(02)00462-4)
- Oyinbo, S. T., Ikumapayi, O. M., Ajiboye, J. S., & Afolalu, S. A. (2015). Numerical Simulation of Axisymmetric and Asymmetric Extrusion Process Using Finite Element Method. *International Journal of Scientific & Engineering Research*, 6(6).
- Rasti, J., Najafizadeh, A., & Meratian, M. (2011). Correcting the stress-strain curve in hot compression test using finite element analysis and Taguchi method. *International Journal of ISSI*, 8(1), 26–33. Retrieved from http://journal.issiran.com/article_6374_44b99e06e066fa7ee24705f05935b39d.pdf
- Rout, A. K., Maity, K., & Sahoo, S. K. (2017). FEM Modeling of Extrusion of Square Billet to Square Product Through Cosine Dies. *Journal of The Institution of Engineers (India): Series C*, 98(2), 91–

96. <https://doi.org/10.1007/s40032-016-0245-x>
- Solomon, N., & Solomon, I. (2010). Effect of die shape on the metal flow pattern during direct extrusion process. *Revista de Metalurgia*, 46(5), 396–404. <https://doi.org/10.3989/revmetalm.0928>
- Zhang, Z. J., Dai, G. Z., Wu, S. N., Dong, L. X., & Liu, L. L. (2009). Simulation of 42CrMo steel billet upsetting and its defects analyses during forming process based on the software DEFORM-3D. *Materials Science and Engineering A*, 499(1–2), 49–52. <https://doi.org/10.1016/j.msea.2007.11.135>



© 2020 by the authors; licensee Growing Science, Canada. This is an open access article distributed under the terms and conditions of the Creative Commons Attribution (CC-BY) license (<http://creativecommons.org/licenses/by/4.0/>).